Human copper transporter 2 is localized in late endosomes and lysosomes and facilitates cellular copper uptake

Peter V.E. van den Berghe, Dineke E. Folmer, Helga E.M. Malingré, Ellen van Beurden, Adriana E.M. Klomp, Bart van de Sluis, Maarten Merkx, Ruud Berger, Leo W.J. Klomp

Biochemical Journal Immediate Publication. Published on 6 Jul 2007 as manuscript BJ20070705

HUMAN COPPER TRANSPORTER 2 IS LOCALIZED IN Llate ENDOSOMES AND LYSOSOMES AND FACILITATES CELLULAR COPPER UPTAKE

Peter V.E van den Berghe[*], Dineke E. Folmer[*], Helga E.M. Malingré[*], Ellen van Beurden[*], Adriana E.M. Klomp[*], Bart van de Sluis[*,†], Maarten Merkx[‡], Ruud Berger[*], Leo W.J. Klomp[*,§]

[*]Department of Metabolic and Endocrine Diseases, University Medical Center Utrecht, 3584 EA Utrecht, The Netherlands, [†]Complex Genetics Section, Department of Medical Genetics, University Medical Center Utrecht, 3508 TA Utrecht, The Netherlands, [‡]Department of Biomedical Engineering, Technical University Eindhoven, 5600 MB Eindhoven, The Netherlands

[§]Address correspondence to: Dr. Leo W.J. Klomp, Department of Metabolic and Endocrine Diseases, University Medical Center Utrecht, Lundlaan 6 (KC-02.069.1), 3584 EA Utrecht, The Netherlands, Tel. (0031) 30 2505318; Fax. (0031) 30 2504295; E-mail: L.Klomp@umcutrecht.nl

Running Title: hCTR2 Facilitates Copper Uptake in Mammalian Cells

ABBREVIATIONS

[#]Abbreviations used: BCS, bathocuproinedisulphonic acid; CTR, copper transporter; D-MEM, Dulbecco's modified Eagle's Medium; DMT1, divalent metal transporter 1; eGFP, enhanced green fluorescent protein; EGS, ethylene glycolbis(succinimidylsuccinate); EV, empty vector; FCS: foetal calf serum; hCTR1, human CTR1; hCTR2, human CTR2; HEK 293T, human embryonic kidney 293T; MEF, mouse embryonic fibroblasts; MRE, metal responsive elements; MTF-I, metal responsive transcriptionfactor I; MRE-Luciferase reporter, pGL3-E1b-TATA-4MRE construct; MTT, Thiazolyl Blue Tetrazolium Bromide; RLU, relative light units; TFR, transferrin receptor; vsvG, vesicular-stomatitis-virus glycoprotein

SYNOPSIS

High affinity cellular copper uptake is mediated by the copper transporter 1 (CTR1) family of proteins. The highly homologous human CTR2 (hCTR2) protein has been identified, but its function in copper uptake is unknown. To characterise the role of hCTR2 in copper homeostasis, epitope-tagged hCTR2 was transiently expressed in different cell lines. hCTR2-vsvG predominantly migrated as a 17-kDa band after immunoblot analysis, consistent with its predicted molecular mass. Chemical cross-linking resulted in detection of higher molecular mass complexes containing hCTR2-vsvG. Furthermore, hCTR2-vsvG was coimmunoprecipitated with hCTR2-flag, suggesting that hCTR2 forms multimers like hCTR1. Transiently transfected hCTR2-eGFP was localized exclusively in late endosomes and lysosomes and was not detected at the plasma membrane. To functionally address the role of hCTR2 in copper metabolism, a novel transcription-based copper sensor was developed. This MRE-Luciferase reporter contained four metal responsive elements (MRE) of the mouse metallothionein 1A promoter upstream of the Firefly Luciferase open reading frame. Thus, the MRE-Luciferase reporter measured bio-available cytosolic copper. Expression of hCTR1 resulted in strong reporter activation, with maximal induction at 1 μM $CuCl_2$, consistent with the K_m of hCTR1. Interestingly, expression of hCTR2 significantly induced MRE-Luciferase reporter activation in a copper-dependent manner at 40 μM and 100 μM $CuCl_2$. Taken together, these data identify hCTR2 as an oligomeric membrane protein localized in lysosomes, which stimulates copper delivery to the cytosol of human cells at relatively high copper concentrations. This work suggests a role of endosomal / lysosomal copper pools in maintaining cellular copper homeostasis.

Keywords: Ctr1, Ctr2, copper uptake, copper bio-sensor, mammalian cells, cellular localisation

INTRODUCTION

Copper is an essential trace element for all organisms that utilize oxygen as electron acceptor during respiration. As a transition metal, copper serves as a cofactor in a number of redox enzymes. The same redox-active properties also render the metal potentially toxic as it can induce free radical formation and confer direct damage to proteins, lipids and DNA. To maintain copper homeostasis, remarkably efficient mechanisms have evolved to regulate copper import, export and cellular distribution of the metal, and the proteins involved in cellular copper homeostasis are largely conserved in prokaryotes and eukaryotes [1-3]. These proteins form intricate metabolic pathways aimed at maintaining an extremely low free copper concentration, while ensuring that sufficient copper is bio-available to sustain essential copper-dependent cellular processes [4]. As one example, a significant proportion of cellular copper is bound to copper chaperones, which deliver copper to specific target enzymes or transporters via regulated protein-protein interactions [5, 6]. As a second example, metallothioneins are small ubiquitously expressed proteins, which scavenge cytosolic copper and other metals like zinc and cadmium [7]. Cells transcriptionally regulate the expression of metallothionein genes in a copper-dependent fashion.

Severe disorders may arise as a result of the disruption of copper homeostasis. Recessive mutations in the gene encoding the P_{1B}-type ATPase ATP7A cause the fatal X-linked neurodevelopmental disorder called Menkes disease [8, 9]. ATP7A deficiency results in a lack of copper transport through the placenta and the intestinal epithelium, leading to systemic copper deficiency and the failure to provide essential cuproenzymes with the metal. The *calamity* mutant of zebrafish (*Danio rerio*) provides a recently characterised animal model for Menkes disease [10]. This mutant displays a marked reduction of pigment formation and a strikingly altered notochord development. Interestingly, the *calamity* mutant is phenocopied by copper deficiency, thus further illustrating the essential role of copper in physiology and development.

Copper uptake is facilitated by the copper transporter $(CTR)^{\#}$ family of proteins that are highly conserved [11]. In *Saccharomyces cerevisiae*, high affinity copper import is mediated by yCtr1 and yCtr3p [12, 13]. A third Ctr protein expressed in *S. cerevisiae*, yCtr2, is thought to mediate low affinity copper import. In mammals, a high affinity copper permease, CTR1, facilitates copper import with a K_m of approximately 1-5 μM [14]. Human CTR1 (hCTR1) is predominantly localized in intracellular vesicles in close apposition to the Golgi-complex, but a fraction is also present at the plasma membrane [15, 16]. The proportion of cell surface exposed hCTR1 is dependent on the cell type [15] and elevated concentrations of copper lead to internalization of cell surface hCTR1, possibly as a rapid adaptive response to limit copper uptake [17]. hCTR1 contains three membrane spanning regions and is thought to assemble into a trimer, thereby forming an aqueous pore to enable copper transport [18, 19].

The physiological role of the Ctr1 family of proteins has been addressed elegantly in knockout mouse models. *Ctr1* knockout mice died during midgestation as a result of copper deficiency [20, 21]. Conditional knockout mice that lack *Ctr1* specifically in the intestinal epithelium were born healthy, but displayed markedly impaired dietary copper uptake, resulting in severe systemic copper deficiency comparable to Menkes disease patients [22]. Together, this work established the essential role of Ctr1 in embryonic development and in dietary copper uptake. However, these animals display some residual cellular copper uptake, suggesting additional pathways of copper import. Furthermore, mouse embryonic fibroblasts (MEFs) obtained from *Ctr1* knockout embryos survived in culture without extra copper added to their media, and these MEFs were able to take up copper in a low affinity manner [23]. The proteins mediating Ctr1-independent low affinity copper import have currently not been characterised.

A candidate protein to participate in such alternative copper import routes is hCTR2. Alignment of the primary amino acid sequences of hCTR1 and CTR2 of multiple species revealed marked homology in the transmembrane regions, suggesting that hCTR2 contains three putative transmembrane regions similar to hCTR1 [14, 24] (Figure 1A). In analogy with hCTR1, the amino-terminus is probably located extracytoplasmically [14, 24]. The highly conserved MXXXM motif (Met-Xaa-Xaa-Xaa-Met) in the second transmembrane region of hCTR1, which has been shown to be critical for copper coordination during copper uptake [25], is also present in hCTR2. All amino acid residues shown to be critical for oligomerisation and copper transport activity of hCTR1 are conserved in hCTR2: the GXXXG (Gly-Xaa-Xaa-Xaa-Gly) motif in the third putative transmembrane region of hCTR1 [26], one methionine residue, approximately 20 residues upstream of the first transmembrane domain (Figure 1A, asterisks) and the MXXXM motif in the second transmembrane domain [27]. There are also notable differences between hCTR2 and hCTR1. Most strikingly, hCTR2 lacks the Mets motifs and Histidine-rich regions that are important for copper transport with high affinity, and does not contain appropriate consensus N-glycosylation sites [27-29]. Taken together, these observations support the copper transport function of hCTR2, but suggest that this occurs with lower affinity than that of hCTR1. However, the function of hCTR2 has not been experimentally addressed and its annotation as a copper transporter has been based only on sequence alignment [30]. Here we characterised the role of hCTR2 in copper homeostasis using a combination of biochemical analyses, cellular localisation studies and a novel copper sensor. The presented data provide evidence that hCTR2 is an intracellular protein involved in copper uptake in human cells.

EXPERIMENTAL

Cell culture and MTT viability assay

The human embryonic kidney 293T (HEK 293T) cell line, the HeLa cell line, and the U2OS cell line were purchased from the A.T.C.C. (Rockville, MD, U.S.A.). Cells were cultured at 37^{o} C under

humidified air containing 5% CO_2, and were maintained in D-MEM Glutamax (Invitrogen, Breda, The Netherlands) containing 10% foetal calf serum (FCS) (Invitrogen), 100 μg/ml penicillin and 100 μg/ml streptomycin (P/S) (Invitrogen). For some experiments, cells were cultured in D-MEM containing 10% FCS and P/S in the presence of different concentrations of $CuCl_2$, $ZnCl_2$, $MgCl_2$, $FeCl_3$, $MnCl_2$ (Merck Chemicals, Amsterdam, The Netherlands), or the copper chelator bathocuproinedisulphonic acid (BCS) (Sigma, Zwijndrecht, The Netherlands). Thiazolyl Blue Tetrazolium Bromide (MTT) viability assays [31] were performed after incubation of the cells with different metal concentrations in 96-well microtiter plates (Corning, Germany). Cells were incubated with 0.4 mg/ml MTT (Sigma) in D-MEM containing 10% FCS and P/S for 30 minutes at 37^{o}C. Prior to lysis, cells were rinsed twice with phosphate buffered saline (PBS; 25 mM sodium phosphate buffer, 140 mM NaCl; pH, 7.4), and cells were lysed in 100 μl 100% iso-propanol containing 40 mM HCl. Conversion into formazan was measured using the multiplate reader model 550 spectrophotometer (Bio-Rad Laboratories B.V., Veenendaal, the Netherlands) at 595 nm and viability was calculated relative to untreated cells.

Plasmids

pCL-NEO RabIP4-vsvG was kindly provided by dr. P.J. van de Sluijs (Department of Cell Biology, UMC Utrecht, the Netherlands). pCDNA3.1-Cullin1-flag was amplified from liver cDNA using flag-cullin fw and rev primers (Table 1). The PCR fragment was cloned into pCRII (Invitrogen), and subsequently cloned into pCDNA31./ZEO. hCTR2-vsvG cDNA was amplified from cDNA by PCR using hCTR2-vsvG fw and hCTR2-vsvG rev primers, and subsequently subcloned into pZeoSV2. The reverse primer contained a sequence to add the vesicular-stomatitis-virus glycoprotein (vsvG) tag at the carboxy-terminus of hCTR2 as described for hCTR1-vsvG [15]. To construct pcDNA3.1/Zeo-hCTR1-vsvG (hCTR1-vsvG) and pcDNA3.1/Zeo-hCTR2-vsvG (hCTR2-vsvG), hCTR1-vsvG and hCTR2-vsvG fragments were isolated from pZeoV2-hCTR1-vsvG [15] or pZeoV2-hCTR2-vsvG after digestion by *Bam*HI and *Xba*I. The fragments were ligated into the *Bam*HI and *Xba*I sites of pcDNA3.1/Zeo (Invitrogen). To generate carboxy-terminal enhanced green fluorescent protein (eGFP) tagged hCTR1 and hCTR2, hCTR1 and hCTR2 fragments were amplified from cDNA by PCR using Advantage cDNA polymerase mix (Clontech, Palo Alto, CA, USA) with hCTR1 fw/rev and hCTR2 fw/rev primers (Table 1). The fragments were ligated into the pCRII-vector using the TA-cloning kit (Invitrogen). hCTR1 and hCTR2 fragments were isolated from pCRII after *Eco*RI digestion and subsequently cloned into the *Eco*RI site of pEGFP-N3 (Clontech), resulting in peGFP-N3-hCTR1 (hCTR1-eGFP) and peGFP-N3-hCTR2 (hCTR-eGFP). To generate the pGL3-E1b-TATA-4MRE construct (MRE-Luciferase reporter), four metal responsive elements (MRE) were amplified by PCR from the 4xMRE(d) construct [7, 32] using 4MRE-F/*Hind*III and 4MRE-R/*Pst*I primers (Table 1). The fragment was digested by *Hind*III and *Pst*I, and subsequently subcloned into

the E1b-TATA pGL3 vector (kindly provided by Dr. Eric Kalkhoven, University Medical Centre Utrecht, The Netherlands). hCTR1 and hCTR2 constructs with a carboxy-terminal flag tag were generated by PCR amplification on hCTR1-vsvG and hCTR2-vsvG template constructs using PFU Turbo polymerase (Stratagene, La Jolla, CA, USA) with hCTR1 *Bam*HI fw and hCTR1 *Not*I rev, and hCTR2 *Bam*HI fw and hCTR2 *Not*I rev primers. These PCR fragments were *Bam*HI and *Not*I digested and fragments were ligated in the *Bam*HI and *Not*I sites of pEBB-flag (kindly provided by Dr. C.S. Duckett, Ann Arbor, MI, USA), resulting in pEBB-hCTR1-flag and pEBB-hCTR2-flag constructs. pEBB-hCTR1-flag IXXXI and pEBB-hCTR2-flag IXXXI were generated by Quickchange mutagenesis (Stratagene) with hCTR1 IXXXI fw/rev and hCTR2 IXXXI fw/rev primers. All constructs were verified by sequence analysis.

Transfection, Chemical Cross-linking, Immunoprecipitation, and Immunoblot analysis

HEK293T cells were transiently transfected with hCTR1-vsvG or hCTR2-vsvG using the calcium phosphate-precipitation protocol [33]. Briefly, the calcium phosphate transfection mix was typically 10% of the tissue culture volume. First, DNA was diluted to a concentration of (maximal) 10 µg/ml in 244 mM $CaCl_2$ solution. Second, the DNA mix was diluted with an equal volume of 2xHBSS (to a final concentration of 6.275 mM Hepes, 190 µM Na_2HPO_4, 68.5 mM NaCl, 122 mM $CaCl_2$; pH, 7.5). After twenty minutes of incubation, the transfection mix was added to the cells, and cells were harvested after two days. Chemical cross-linking was performed by incubation of transfected HEK293T cells for 30 minutes at room temperature with PBS containing 1% DMSO in the absence or presence of different concentrations of ethylene glycolbis(succinimidylsuccinate) (EGS) (Pierce Biotechnology Inc, Rockford, IL, USA). For cross-linking experiments and immunoprecipitation, HEK293T cells were lysed in RIPA buffer (50 mM Tris-HCl, 0.1% SDS, 1% Nonidet P-40, 150 mM NaCl, 10 mg/ml sodiumdeoxychalate, 2mM EDTA, 1 mM $NaVO_3$; pH,7.4) supplemented with complete protease inhibitor cocktail (Roche, Woerden, The Netherlands), and shearing seven times through a 23G needle solubilised lysates. For immunoprecipitation, 1 mg of total protein, 20 µl protein-A agarose beads (Sigma) and 0.6 µg rabbit-anti-vsvG antibody (Abcam, Cambridge, UK) were incubated overnight at 4 ^{o}C in a volume of 500 µl while rotating. For co-immunoprecipitation experiments, 1 ml lysate was divided over two precipitation reactions with either 20 µl protein-A agarose beads (Sigma) and 0.6 µg rabbit-anti-vsvG antibody or 20 µl anti-flag M2-agarose (Sigma), which were incubated for 4 hours at 4 ^{o}C in a volume of 500 µl while rotating. Immunocomplexes were precipitated by microcentrifugation at 2000xg and rinsed four times in RIPA buffer. Immunoprecipitates were resuspended in SDS-PAGE sample buffer (62.5 mM Tris-HCl, 4% SDS, 5% glycerol, 0.01% bromophenol blue, 2% β-mercaptoethanol; pH,6.8) and heated at 95^{o}C for 5 minutes prior to separation by SDS-12% PAGE. Proteins were transferred to Hybond-P PVDF membranes (Amersham Biosciences, Buckinghamshire, UK) by standard immunoblot procedures.

The membranes were blocked in Tris buffered saline (TBS; 25 mM Tris-HCl, 137 mM NaCl, 2.7 mM KCl; pH,7.4) containing 5% non-fat dried milk (Sigma) and 0.1% Tween-20. Immunoblots were probed with rabbit-anti-vsvG antibodies (0.6 μg/ml; Abcam), mouse-anti-vsvG hybridoma supernatant from clone P5D4 (1:250 dilution)[24] or mouse- anti-flag M2-peroxidase conjugate (Sigma) for 1 hour. Reactivity was detected using horseradish peroxidase-conjugated secondary antibodies (1 ng/ml; Pierce) and chemoluminescence (ECL^{TM}; Amersham), according to the manufacturer's instructions.

Indirect Immunofluorescence and Confocal Laser Scanning Microscopy

HEK 293T cells, U2OS cells, and HeLa cells were transiently transfected with hCTR1-eGFP, hCTR2-eGFP or hCTR2-vsvG using Lipofectamin2000 according to the manufacturer's protocol (Invitrogen). One day after transfection, cells were trypsinised and seeded on coverslips (Marienfeld, Paul GmbH & Co.KG, Bad Bergentheim, Germany). After 24 hours, cells were rinsed with ice-cold PBS and fixed in PBS, 3.7 % paraformaldehyde for 20 minutes at 4 ^{o}C. Cells were rinsed 3 times with PBS containing 0.02% Triton X-100, and non-specific binding was blocked with blocking buffer (5% BSA in PBS, 0.02% Triton X-100) for 30 minutes at room temperature. Immunolabelling was performed in blocking buffer for one hour with the antibodies indicated below. Cells were rinsed three times with PBS, 0.02% Triton X-100, and secondary labelling was performed with affinipure goat-anti-mouse or goat-anti-rabbit IgG (H+L) antibodies (10 μg/ml; Molecular Probes, Eugene, OR, U.S.A.). Coverslips were mounted in Fluorsave (VWR International Ltd, Leicestershire, UK), and confocal laser scanning microscopy (Leica TCS 4D, Rijswijk, The Netherlands) was performed using dedicated imaging software. hCTR1-vsvG and hCTR2-vsvG were labelled with rabbit-anti-vsvG antibodies (0.6 μg/ml; Abcam). For double-labelling experiments, monoclonal antibodies against trans-Golgi network (TGN) 230-kDa protein (p230) (1.25 μg/ml; BD Biosciences), human transferrin receptor (TFR) (1 μg/ml; Molecular Probes) late endosomal marker CD63 (75 ng/ml; Zymed Laboratories Inc., San Francisco, CA, USA), and lysosomal markers CD107a (LAMP-1) and CD107b (LAMP-2) (5 μg/ml; BD Biosciences) were used.

Luciferase Reporter Assays

For Luciferase reporter assays HEK 293T cells were seeded in 96-wells plates and transiently transfected using the calcium phosphate-transfection protocol. Each well was co-transfected with 35 ng of MRE-Luciferase reporter, 0.25 ng pRL-TK Vector (Promega Benelux BV, Leiden, the Netherlands), and 3.5 ng of hCTR1-vsvG or hCTR2-vsvG, or 0.35 ng pEBB-hCTR1-flag or pEBB-hCTR2-flag constructs as indicated in the figure legends. The next day, cells were rinsed with PBS and subsequently maintained for 24 hours in D-MEM in absence or presence of different metals. For hypoxia response analysis, 10 ng of the hypoxia-responsive reporter vector with 5xHRE [34], and

0.25 ng pRL-TK vector were transiently transfected. Next day, cells were incubated for 24 hours with 100 μM of the iron chelator desferoxamine (DFO). After incubation, cells were rinsed in PBS, harvested in passive lysisbuffer according to the manufacturer's protocol (Promega) and assayed by luminometry (Berthold Technologies, Vilvoorde, Belgium) for Firefly Luciferase activity and Renilla Luciferase activity according to the manufacturer's protocol (Promega; Dual-Luciferase Reporter Assay System). The relative light units (RLU) were calculated by dividing Firefly Luciferase by Renilla Luciferase values. All values were expressed as fold inductions relative to empty vector control incubations (set at 1). Statistical analysis was performed on RLU data for the different incubations. A two-tailed student-T-test was used to analyse statistical differences between different data points.

RESULTS

Biochemical characterisation of hCTR2

To characterise hCTR2, hCTR1-vsvG and hCTR2-vsvG were expressed in HEK293T cells, immunoprecipitated and subjected to immunoblot analysis. No precipitated proteins could be detected in empty vector-transfected cells, whereas hCTR1-vsvG migrated at approximately 35 kDa (Figure 1B). This was consistent with previous studies [15], indicating that the fully glycosylated mature hCTR1 was expressed. hCTR2-vsvG was detected at approximately 17 kDa apparent molecular mass (Figure 1B), in agreement with its size predicted from amino acid sequence analysis (17,000 Da). Crude cell fractionation indicated that hCTR2 was associated with cellular membranes (data not shown). This biochemical analysis indicated that hCTR2-vsvG was expressed as a stable membrane protein and was most probably not glycosylated.

Chemical cross-linking and 2D-crystallography experiments previously revealed that hCTR1 assembles as a trimer [16, 18]. Thus, we considered the possibility that hCTR2 also exists in an oligomeric complex. The amine-reactive chemical cross-linker EGS was used to covalently link cellular interacting proteins. Chemical cross-linking with EGS in HEK 293T cells transiently transfected with hCTR2-vsvG resulted in detection of discrete vsvG immunopositive bands, which migrated at apparent M_r of approximately 24,000 and 35,000. The intensity of these putative hCTR2-vsvG oligomers increased in an EGS concentration-dependent manner (Figure 1C; arrows). At high EGS (1 mM) concentrations, additional complexes of even higher M_r (> 200,000) appeared (data not shown). These data suggested that hCTR2 may be part of oligomeric complexes similar to hCTR1 [16].

To further investigate this possibility, hCTR2 constructs were generated with a carboxy-terminal flag-tag. These constructs were co-expressed with hCTR2-vsvG in HEK 293T cells and cell lysates were subjected to co-immunoprecipitation with either anti-flag M2-agarose beads or protein A agarose beads coupled to rabbit-anti-vsvG antibodies. Immunoprecipitation of both vsvG (Figure 1D,

lanes 7-9) and flag (Figure 1D, lanes 4-6) tagged proteins was observed. Co-immunoprecipitation of hCTR2-vsvG with hCTR2-flag was observed (Figure 1D, lane 1), but no interaction was noted with the small GTPase RabIP4-vsvG (Figure 1D, lane 2), and with Cullin1-flag (Figure 1D, lane 3), which were used as negative controls. Taken together, these experiments suggest that hCTR2 monomers mutually interact, and supports the model that CTR proteins form trimeric complexes to enable copper transport.

Intracellular localisation of hCTR2

To investigate the cellular localisation of hCTR2, we generated constructs encoding hCTR2 with a carboxy-terminal eGFP-tag. Similar to hCTR2-vsvG, hCTR2-eGFP expressed in HEK 293T cells also migrated at its expected molecular weight of 40,000, and could be detected in higher molecular weight oligomers (data not shown). The cellular localisation of hCTR2 was determined after transient transfection of hCTR2-eGFP in HEK 293T cells, U2OS cells and HeLa cells (Figure 2A). hCTR2-eGFP was not detected at the plasma membrane, but was primarily localized in relatively large vesicles in all three cell types (Figure 2A). We set out to exclude the possibility that the inserted tag could have interfered with the localisation of transiently expressed hCTR2. Independently transfected hCTR2-vsvG and hCTR2-flag were also detected in large vesicular compartments in multiple cell types (data not shown) and co-expression of hCTR2-vsvG and hCTR2-eGFP resulted in strong co-localisation (Figure 2B). The latter indicated that the cellular localisation of hCTR2 was independent of the used tag.

Consistent with previous data, hCTR1-eGFP in HeLa cells was detectable at the plasma membrane but was primarily localized in intracellular vesicles, and partly colocalized with hCTR2 (Figure 3A) [15, 16]. Cell surface hCTR1 is known to be rapidly and specifically internalized upon incubation of HEK 293T cells with increased copper concentrations [17]. To determine whether copper affects hCTR2 localisation, HEK 293T cells were transiently transfected with hCTR2-eGFP. Cells were incubated with different copper concentrations or the copper chelating agent bathocuproine disulphonate (BCS) for one hour. No apparent copper-dependent relocalisation of hCTR2 was observed (Figure 3B), which is in concordance with the inability to detect copper-dependent relocalisation of the intracellular fraction of hCTR1 [15].

The nature of the vesicular localisation of hCTR2 in HEK 293T cells was further investigated. HEK 293T cells were transiently transfected with hCTR2-eGFP, and immunofluorescent labelling of different cellular marker proteins was performed. No significant co-localisation was observed between hCTR2-eGFP and an early endosomal marker, the transferrin receptor (TFR), nor between hCTR2-eGFP and the trans-Golgi-complex resident protein p230 (Figure 4). However, hCTR2 partly co-localized with late endosomes labelled by anti-CD63 antibody, and marked co-localisation was observed with the lysosomal markers LAMP-1 and LAMP-2 (Figure 4, arrowheads). Similar results

were observed in HeLa cell (data not shown), indicating that this localisation of hCTR2 in late endosomes and lysosomes was not cell-type specific.

A novel transcription-based copper sensor to measure cytosolic bio-available copper pools

To address whether hCTR2 could facilitate copper uptake, a novel transcription-based copper sensor was designed. The design of this sensor was based on the endogenous capacity of cells to transactivate metallothionein genes in response to elevated cytosolic copper availability. Increase of copper in the cytosol results in the displacement of zinc from metallothioneins. The released zinc binds to and activates the metal responsive transcription factor I (MTF-I), which subsequently induces gene expression by binding to MREs in the promoter region of specific genes [7, 35]. Four metal response elements (MRE) from the murine metallothionein Ia promotor [7, 32] were cloned upstream of the Firefly Luciferase open reading frame in the pGL3-E1b-TATA vector (schematic representation in Figure 5A), resulting in the MRE-Luciferase reporter. A construct encoding the metal-insensitive TK-Renilla Luciferase was used to correct for differences in transfection efficiencies. Similar to the endogenous metallothionein 1A promoter, the MRE-Luciferase reporter was predicted to be transactivated in a metal concentration-dependent fashion by MTF-I [7]. In this way, the MRE-Luciferase reporter measured bio-available cytosolic copper. To test the validity of this approach, the MRE-Luciferase reporter was transiently transfected into HEK 293T cells (Fig 5C) and U2OS cells (data not shown), and cells were incubated with different copper concentrations for 24 hours. At normal copper concentration in the medium, reporter activity was slightly increased compared to cells transfected with a control vector containing no MREs. A linear concentration-dependent induction of MRE-Luciferase reporter activity was noted when cells were incubated with $CuCl_2$ concentrations starting at 20 μM up till 100 μM, an effect that was not observed in empty vector transfected cells (Figure 5C). The induction of the MRE-Luciferase reporter activity was approximately 5-fold at this concentration, and higher concentrations of copper did not result in further induction. More detailed examination of MRE-Luciferase reporter activities at low copper concentrations revealed that the sensor was not effectively induced by copper concentrations below 20 μM in these cells (data not shown). Since the reporter is responsive to cytosolic copper, an increase in reporter activity was interpreted as an indication that copper import and transport over a cellular membrane had in fact occurred. Quantitative RT-PCR experiments revealed induction of the endogenous metallothionein 1A promoter at the same copper concentrations (data not shown). As different metals are known to induce MTF-I mediated transcription [7], the specificity of the MRE-Luciferase reporter for several other biologically important metals was tested. Especially zinc is relevant in this respect, since activation of MTF-I is caused by incorporation of cellular zinc into MTF-I after displacement of zinc from metallothioneins by other metals, such as copper [7]. Initially, metal toxicity was determined by MTT viability assays to calculate LD_{50} values in our cells (Figure 5B). Next, HEK 293T cells were transiently transfected with the MRE-Luciferase reporter, and one

day after transfection cells were incubated with low or high metal concentrations that were still well below lethal concentrations (Figure 5D). $CuCl_2$ and $ZnCl_2$ resulted in induction of reporter activities in a concentration-dependent manner, whereas $MgCl_2$, $FeCl_3$, and $MnCl_2$ failed to activate the MRE-Luciferase reporter. MTF-I-mediated transcription may also be induced by oxidative stress and hypoxia [7, 36]. However, no MRE-Luciferase reporter induction by oxidative stress by incubation with 100 μM hydrogen peroxide or 100 μM paraquat for 24 hours was observed (data not shown) [37]. To mimic hypoxia, cells were treated with the iron chelator desferoxamine (DFO)[38], which resulted in induction of the hypoxia-responsive 5xHRE reporter (Figure 5E). The MRE-Luciferase reporter was only slightly induced upon DFO treatment, whereas $CuCl_2$ strongly induced the MRE reporter but not the 5xHRE reporter (Figure 5D). Taken together with the notion that all experiments in this work were performed under normoxic conditions, we conclude that the MRE-Luciferase reporter specifically determines elevated copper and zinc concentrations in these defined experimental conditions.

hCTR1 and hCTR2 facilitate copper uptake

Next, we tested if this approach could be used to effectively assess perturbations in the known copper import pathway. Towards this end, hCTR1-flag was co-transfected into HEK 293T cells together with the MRE-Luciferase reporter. Without additional $CuCl_2$ added to the medium this resulted in a significant increase of reporter activity of approximately 3-fold compared to empty vector transfected cells (Figure 6A and 6B). This increase could be completely prevented by incubation with the copper chelator BCS (data not shown), indicating that exogenous expression of hCTR1-flag resulted in significantly increased cytosolic copper at the low copper concentration in the cell culture medium. Further addition of $CuCl_2$ up to 2.5 μM resulted in marked and significant increase of reporter activity with a maximal 10-fold induction (Figure 6A). Since the MRE-Luciferase reporter was activated by zinc as well as by copper, one possible explanation for the reporter induction would be that exogenous expression of hCTR1-flag resulted in mobilisation of sequestered vesicular zinc pools under conditions of excess copper. To address this possibility, the effects of transient transfection of hCTR1-flag on the zinc-induced reporter activity were assessed. In empty vector transfected cells, no induction of MRE-Luciferase reporter activity was observed upon incubation with $ZnCl_2$ at the same concentrations as used in the copper experiments. In cells expressing exogenous hCTR1-flag, the basal reporter activity was raised approximately 3-fold similarly as shown before (cf. Figure 6A and Figure 6B), but the MRE-Luciferase activity was not further induced as a result of additional $ZnCl_2$ (Figure 6B), strongly indicating that expression of hCTR1-flag resulted in increased bioavailability of copper, but not zinc. As a control, immunoblot analysis of hCTR1-flag was used to determine protein expression under these conditions (Figure 6E). Together, these data indicated the feasibility to use the MRE-Luciferase reporter to specifically assess changes in the expression of copper import proteins on copper uptake. Furthermore, these data

underscored previous observations that expression of hCTR1 was a limiting factor in copper import, at least at relatively low copper concentrations [14].

Next, the potential role of hCTR2 in copper import was studied in a similar manner by co-transfection of constructs encoding hCTR2-flag together with the MRE-Luciferase reporter in HEK 293T cells. Expression of hCTR2-flag was verified by immunoblot analysis (Figure 6E). In empty vector-transfected cells, reporter activity was induced starting at 10-20 μM $CuCl_2$ (data not shown). However, hCTR2-flag expression resulted in a significantly higher reporter induction compared to empty vector transfected cells. At 40 μM $CuCl_2$, and at 100 μM $CuCl_2$, expression of hCTR2-flag resulted in a > 2-fold increase (Figure 6C). The increased hCTR2-flag-dependent MRE-Luciferase reporter activation was copper specific, as no differences were observed upon incubation with $ZnCl_2$ (Figure 6D). To further demonstrate that the function of hCTR2 was copper-specific, we mutated the methionine residues in the MXXXM motif to isoleucines. Previous findings by Eisses *et al*. revealed a marked reduction of hCTR1-mediated copper uptake after disruption of the analogous methionines of hCTR1 [25]. Whereas expression of wildtype hCTR1-flag or hCTR2-flag resulted in a significant copper-dependent induction of the MRE-Luciferase reporter, substitution of the MXXXM motifs to IXXXI completely abolished reporter induction by hCTR1-flag and by hCTR2-flag (Figures 6A and 6C), while all proteins were expressed (Figure 6E). No differences were observed after incubation with $ZnCl_2$ (Figures 6B and 6D). Taken together, expression of hCTR2 facilitates cellular copper uptake with a lower affinity compared to hCTR1.

DISCUSSION

Since the initial characterisation of hCTR1 almost a decade ago [30], elegant studies have addressed the structure and localisation of mammalian Ctr1, its transport kinetics, its regulation by copper and its role in embryonic development and dietary copper uptake in mice [14-18, 20-27, 29, 39, 40]. While these studies have greatly increased our knowledge of the mechanisms of cellular copper uptake, they also established that Ctr1-independent copper import pathways exist. MEFs obtained from *Ctr1* knockout embryos indeed displayed low affinity copper uptake [23]. Based on the evidence presented here, we propose that hCTR2, a protein with structural similarity to hCTR1 but with a previously unknown function, mediates such an alternative low-affinity copper import pathway in human cells.

To be able to characterise the function of hCTR2, we constructed a novel metal sensor. This sensor allowed sensitive and high-throughput assessment of copper homeostasis. It is important to notice that the MRE-Luciferase reporter measures cytosolic bio-available copper and is based on a cell intrinsic copper sensing mechanism without the necessity to add exogenous compounds that directly bind copper and might potentially interfere with the copper homeostatic mechanisms present in the cell [41]. By performing control experiments with zinc, the sensor enabled us to determine the

specific effects of exogenously expressed proteins on copper metabolism. Our data strongly indicate that hCTR2 facilitates cellular copper import with a lower affinity than that mediated by hCTR1. At copper concentrations below 10 μM, at which hCTR1-dependent MRE-Luciferase reporter activity was maximally induced, no effects of hCTR2 expression on reporter activity could be detected. In contrast, exogenous expression of hCTR2 resulted in significantly higher copper-dependent MRE-Luciferase activity compared to empty vector controls. This effect was copper-specific, since mutation of conserved methionine residues known to be essential for copper transport in CTR proteins completely abolished activation of the reporter. Therefore, hCTR2 expression resulted in a specific increase of cytosolic copper availability at high concentrations. Since the copper sensor does not directly measure transport, further studies are necessary to address the kinetics of hCTR2-mediated copper import in more detail.

The apparent steady state localisation of this protein in the endosomal-lysosomal compartment is notable. Lysosomes in mammalian cells and the vacuoles in yeast have equivalent functions. In baker's yeast *S. cerevisiae*, the hCTR2 orthologue yCtr2p is localized in the vacuolar membrane and can mobilize vacuolar copper pools [42]. A similar vacuolar membrane localisation was observed for Ctr6, the hCTR2 orthologue in fission yeast *S. pombe* [43]. Combined with our data, we suggest that endosomal-lysosomal localisation and mobilisation of intracellular copper stores are common properties of yeast and mammalian CTR2/Ctr6 proteins. In our opinion, the observed intracellular localisation of hCTR2 is correct, since it was observed in multiple cell types and appeared independent of the tags used. Moreover, expressed proteins indeed stimulated functional copper uptake activity. A similar localisation of endogenous CTR2 in large vesicular compartments reminiscent of late endosomes and lysosomes was observed in human and monkey cells in independent studies (J. Bertinato et al., personal communication). There is ample precedence for the localisation of copper transporters in intracellular compartments. Under basal copper levels, the copper-transporting P-type ATPase ATP7A resides in the Golgi compartment and is only distributed towards peripheral vesicles and the plasmamembrane upon increased cytosolic copper concentrations [44, 45]. In addition, hCTR1 also resides predominantly in intracellular vesicles, but has been shown to recycle constitutively with the plasma membrane [17, 24]. In fact, part of the intracellular hCTR2 resided in vesicular compartments that also contained hCTR1, but further studies are required to clarify the implications of this intriguing observation.

Our data suggest that hCTR2 is an intracellular, oligomeric membrane protein, which is rate limiting for the delivery of copper to the cytosol at high copper concentrations. Below we attempt to integrate these findings into a model of cellular copper uptake by hCTR2. In mammalian cells, extracellular copper and cuproenzymes destined for lysosomal degradation may be endocytosed or pinocytosed by CTR-dependent or CTR-independent mechanisms. Copper may subsequently be concentrated in lysosomes, prior to mobilisation by hCTR2. This process may require high extracellular concentrations of copper or prolonged concentration of copper in lysosomal vesicles,

consistent with our observation that hCTR2 stimulates copper uptake at relative copper excess. This model fits with current knowledge on the biology of dietary copper import and intracellular copper sequestration. Intestinal epithelium of gut-specific *Ctr1* null mice unexpectedly accumulated dietary copper [22]. The failure to express Ctr1 did therefore not lead to reduced cellular copper uptake, but rather resulted in increased intracellular sequestration of copper, presumably in lysosomal vesicles. If, in analogy with our observations, mouse Ctr2 would indeed function to mobilize copper from intracellular pools in gut epithelium, this activity is clearly not sufficient to prevent the severe systemic copper deficiency in intestine-specific *Ctr1* null mice [22]. Although the existence of vesicular copper stores in mammalian cells remains speculative, extensive copper accumulation has indeed been observed in lysosomes of Wilson disease patients [46], in LEC rats, a model for Wilson disease [47] and in liver cells of Bedlington terriers affected with copper toxicosis [48]. Finally, several other metal transport systems utilize the endocytic machinery to import metals into the cytosol. In yeast, zinc transporters regulate vacuolar zinc stores to modulate zinc homeostasis [49]. Mouse zinc transporter ZIP1, ZIP3, and ZIP4 are localized in intracellular vesicles, and may translocate to the plasma membrane for zinc uptake [50, 51]. Furthermore, the divalent metal transporter 1 (DMT1) protein is involved in the transfer of endocytosed iron into the cytosol [52, 53]. Therefore, cellular copper uptake may require a combination of transport over the plasma membrane, endocytosis of the metal and mobilisation from intracellular pools, in analogy to the uptake of other transition metals.

In summary, these data suggest that hCTR2 is predominantly localized in the endosomal system and stimulates copper uptake with a relatively low affinity to make it bio-available in the cytosol, and suggest that hCTR2 may be responsible for the residual copper uptake activity observed in cells obtained from *Ctr1* null embryos. Since this work comprises the first study on the function and localisation of hCTR2, many questions remain unanswered. It will be important to further study the nature and function of vesicular copper sequestration in copper homeostasis and to identify the mechanisms that are responsible for import of copper into the endosomal-lysosomal system. Ultimately, studying the impact of knocking out Ctr2 from the mouse genome on copper homeostasis at the level of the entire organism will be required to obtain a complete understanding of the regulation of copper uptake under different conditions and cellular demands.

REFERENCES

1 Culotta, V. C., Lin, S. J., Schmidt, P., Klomp, L. W., Casareno, R. L. and Gitlin, J. (1999) Intracellular pathways of copper trafficking in yeast and humans. Adv. Exp. Med. Biol. **448**, 247-254

2 de Bie, P., van de Sluis, B., Klomp, L. and Wijmenga, C. (2005) The many faces of the copper metabolism protein MURR1/COMMD1. J. Hered. **96**, 803-811

3 Himelblau, E. and Amasino, R. M. (2000) Delivering copper within plant cells. Curr. Opin. Plant. Biol. **3**, 205-210

4 Rae, T. D., Schmidt, P. J., Pufahl, R. A., Culotta, V. C. and O'Halloran, T. V. (1999) Undetectable intracellular free copper: the requirement of a copper chaperone for superoxide dismutase. Science **284**, 805-808

5 Casareno, R. L., Waggoner, D. and Gitlin, J. D. (1998) The copper chaperone CCS directly interacts with copper/zinc superoxide dismutase. J. Biol. Chem. **273**, 23625-23628

6 Hamza, I., Schaefer, M., Klomp, L. W. and Gitlin, J. D. (1999) Interaction of the copper chaperone HAH1 with the Wilson disease protein is essential for copper homeostasis. Proc. Natl. Acad. Sci. U S A **96**, 13363-13368

7 Zhang, B., Georgiev, O., Hagmann, M., Gunes, C., Cramer, M., Faller, P., Vasak, M. and Schaffner, W. (2003) Activity of metal-responsive transcription factor 1 by toxic heavy metals and H2O2 in vitro is modulated by metallothionein. Mol. Cell. Biol. **23**, 8471-8485

8 Mercer, J. F., Livingston, J., Hall, B., Paynter, J. A., Begy, C., Chandrasekharappa, S., Lockhart, P., Grimes, A., Bhave, M., Siemieniak, D. and et al. (1993) Isolation of a partial candidate gene for Menkes disease by positional cloning. Nat. Genet. **3**, 20-25

9 Vulpe, C., Levinson, B., Whitney, S., Packman, S. and Gitschier, J. (1993) Isolation of a candidate gene for Menkes disease and evidence that it encodes a copper-transporting ATPase. Nat. Genet. **3**, 7-13

10 Mendelsohn, B. A., Yin, C., Johnson, S. L., Wilm, T. P., Solnica-Krezel, L. and Gitlin, J. D. (2006) Atp7a determines a hierarchy of copper metabolism essential for notochord development. Cell Metab. **4**, 155-162

11 Petris, M. J. (2004) The SLC31 (Ctr) copper transporter family. Pflugers Arch. **447**, 752-755

12 Dancis, A., Yuan, D. S., Haile, D., Askwith, C., Eide, D., Moehle, C., Kaplan, J. and Klausner, R. D. (1994) Molecular characterization of a copper transport protein in S. cerevisiae: an unexpected role for copper in iron transport. Cell **76**, 393-402

13 Knight, S. A., Labbe, S., Kwon, L. F., Kosman, D. J. and Thiele, D. J. (1996) A widespread transposable element masks expression of a yeast copper transport gene. Genes Dev. **10**, 1917-1929

14 Eisses, J. F. and Kaplan, J. H. (2002) Molecular characterization of hCTR1, the human copper uptake protein. J. Biol. Chem. **277**, 29162-29171

15 Klomp, A. E., Tops, B. B., Van Denberg, I. E., Berger, R. and Klomp, L. W. (2002) Biochemical characterization and subcellular localization of human copper transporter 1 (hCTR1). Biochem. J. **364**, 497-505

16 Lee, J., Pena, M. M., Nose, Y. and Thiele, D. J. (2002) Biochemical characterization of the human copper transporter Ctr1. J. Biol. Chem. **277**, 4380-4387

17 Petris, M. J., Smith, K., Lee, J. and Thiele, D. J. (2003) Copper-stimulated endocytosis and degradation of the human copper transporter, hCtr1. J Biol. Chem. **278**, 9639-9646

18 Aller, S. G. and Unger, V. M. (2006) Projection structure of the human copper transporter CTR1 at 6-A resolution reveals a compact trimer with a novel channel-like architecture. Proc. Natl. Acad. Sci. U S A **103**, 3627-3632

19 Nose, Y., Rees, E. M. and Thiele, D. J. (2006) Structure of the Ctr1 copper trans'PORE'ter reveals novel architecture. Trends Biochem. Sci. **31**, 604-607

20 Lee, J., Prohaska, J. R. and Thiele, D. J. (2001) Essential role for mammalian copper transporter Ctr1 in copper homeostasis and embryonic development. Proc. Natl. Acad. Sci. U S A **98**, 6842-6847

21 Kuo, Y. M., Gybina, A. A., Pyatskowit, J. W., Gitschier, J. and Prohaska, J. R. (2006) Copper transport protein (Ctr1) levels in mice are tissue specific and dependent on copper status. J. Nut.r **136**, 21-26

22 Nose, Y., Kim, B. E. and Thiele, D. J. (2006) Ctr1 drives intestinal copper absorption and is essential for growth, iron metabolism, and neonatal cardiac function. Cell Metab. **4**, 235-244

23 Lee, J., Petris, M. J. and Thiele, D. J. (2002) Characterization of mouse embryonic cells deficient in the ctr1 high affinity copper transporter. Identification of a Ctr1-independent copper transport system. J. Biol. Chem. **277**, 40253-40259

24 Klomp, A. E., Juijn, J. A., van der Gun, L. T., van den Berg, I. E., Berger, R. and Klomp, L. W. (2003) The N-terminus of the human copper transporter 1 (hCTR1) is localized extracellularly, and interacts with itself. Biochem. J. **370**, 881-889

25 Eisses, J. F. and Kaplan, J. H. (2005) The mechanism of copper uptake mediated by human CTR1: a mutational analysis. J. Biol. Chem. **280**, 37159-37168

26 Aller, S. G., Eng, E. T., De Feo, C. J. and Unger, V. M. (2004) Eukaryotic CTR copper uptake transporters require two faces of the third transmembrane domain for helix packing, oligomerization, and function. J. Biol. Chem. **279**, 53435-53441

27 Puig, S., Lee, J., Lau, M. and Thiele, D. J. (2002) Biochemical and genetic analyses of yeast and human high affinity copper transporters suggest a conserved mechanism for copper uptake. J. Biol. Chem. **277**, 26021-26030

28 Pena, M. M., Lee, J. and Thiele, D. J. (1999) A delicate balance: homeostatic control of copper uptake and distribution. J. Nutr. **129**, 1251-1260

29 Puig, S. and Thiele, D. J. (2002) Molecular mechanisms of copper uptake and distribution. Curr. Opin. Chem. Biol. **6**, 171-180

30 Zhou, B. and Gitschier, J. (1997) hCTR1: a human gene for copper uptake identified by complementation in yeast. Proc. Natl. Acad. Sci. U S A **94**, 7481-7486

31 Mosmann, T. (1983) Rapid colorimetric assay for cellular growth and survival: application to proliferation and cytotoxicity assays. J. Immunol. Methods **65**, 55-63

32 Westin, G., Gerster, T., Muller, M. M., Schaffner, G. and Schaffner, W. (1987) OVEC, a versatile system to study transcription in mammalian cells and cell-free extracts. Nucleic Acids Res. **15**, 6787-6798

33 de Bie, P., van de Sluis, B., Burstein, E., Duran, K. J., Berger, R., Duckett, C. S., Wijmenga, C. and Klomp, L. W. (2006) Characterization of COMMD protein-protein interactions in NF-kappaB signalling. Biochem. J. **398**, 63-71

34 Shibata, T., Giaccia, A. J. and Brown, J. M. (2000) Development of a hypoxia-responsive vector for tumor-specific gene therapy. Gene Ther. **7**, 493-498

35 Palmiter, R. D. (1994) Regulation of metallothionein genes by heavy metals appears to be mediated by a zinc-sensitive inhibitor that interacts with a constitutively active transcription factor, MTF-1. Proc. Natl. Acad. Sci. U S A **91**, 1219-1223

36 Murphy, B. J., Andrews, G. K., Bittel, D., Discher, D. J., McCue, J., Green, C. J., Yanovsky, M., Giaccia, A., Sutherland, R. M., Laderoute, K. R. and Webster, K. A.

(1999) Activation of metallothionein gene expression by hypoxia involves metal response elements and metal transcription factor-1. Cancer Res. **59**, 1315-1322

37 Poss, K. D. and Tonegawa, S. (1997) Reduced stress defense in heme oxygenase 1-deficient cells. Proc Natl Acad Sci U S A **94**, 10925-10930

38 Bianchi, L., Tacchini, L. and Cairo, G. (1999) HIF-1-mediated activation of transferrin receptor gene transcription by iron chelation. Nucleic Acids Res. **27**, 4223-4227

39 Eisses, J. F., Chi, Y. and Kaplan, J. H. (2005) Stable plasma membrane levels of hCTR1 mediate cellular copper uptake. J. Biol. Chem. **280**, 9635-9639

40 Kuo, Y. M., Zhou, B., Cosco, D. and Gitschier, J. (2001) The copper transporter CTR1 provides an essential function in mammalian embryonic development. Proc. Natl. Acad. Sci. U S A **98**, 6836-6841

41 Zeng, L., Miller, E. W., Pralle, A., Isacoff, E. Y. and Chang, C. J. (2006) A selective turn-on fluorescent sensor for imaging copper in living cells. J. Am. Chem. Soc. **128**, 10-11

42 Rees, E. M., Lee, J. and Thiele, D. J. (2004) Mobilization of intracellular copper stores by the ctr2 vacuolar copper transporter. J. Biol. Chem. **279**, 54221-54229

43 Bellemare, D. R., Shaner, L., Morano, K. A., Beaudoin, J., Langlois, R. and Labbe, S. (2002) Ctr6, a vacuolar membrane copper transporter in Schizosaccharomyces pombe. J. Biol. Chem. **277**, 46676-46686

44 Petris, M. J., Mercer, J. F., Culvenor, J. G., Lockhart, P., Gleeson, P. A. and Camakaris, J. (1996) Ligand-regulated transport of the Menkes copper P-type ATPase efflux pump from the Golgi apparatus to the plasma membrane: a novel mechanism of regulated trafficking. Embo J. **15**, 6084-6095

45 Yamaguchi, Y., Heiny, M. E., Suzuki, M. and Gitlin, J. D. (1996) Biochemical characterization and intracellular localization of the Menkes disease protein. Proc. Natl. Acad. Sci. U S A **93**, 14030-14035

46 Sternlieb, I., Van den Hamer, C. J., Morell, A. G., Alpert, S., Gregoriadis, G. and Scheinberg, I. H. (1973) Lysosomal defect of hepatic copper excretion in Wilson's disease (hepatolenticular degeneration). Gastroenterology **64**, 99-105

47 Terada, K., Aiba, N., Yang, X. L., Iida, M., Nakai, M., Miura, N. and Sugiyama, T. (1999) Biliary excretion of copper in LEC rat after introduction of copper transporting P-type ATPase, ATP7B. FEBS Lett. **448**, 53-56

48 Haywood, S., Fuentealba, I. C., Foster, J. and Ross, G. (1996) Pathobiology of copper-induced injury in Bedlington terriers: ultrastructural and microanalytical studies. Anal. Cell Pathol. **10**, 229-241

49 MacDiarmid, C. W., Gaither, L. A. and Eide, D. (2000) Zinc transporters that regulate vacuolar zinc storage in Saccharomyces cerevisiae. Embo J. **19**, 2845-2855

50 Kim, B. E., Wang, F., Dufner-Beattie, J., Andrews, G. K., Eide, D. J. and Petris, M. J. (2004) Zn2+-stimulated endocytosis of the mZIP4 zinc transporter regulates its location at the plasma membrane. J. Biol. Chem. **279**, 4523-4530

51 Wang, F., Dufner-Beattie, J., Kim, B. E., Petris, M. J., Andrews, G. and Eide, D. J. (2004) Zinc-stimulated endocytosis controls activity of the mouse ZIP1 and ZIP3 zinc uptake transporters. J. Biol. Chem. **279**, 24631-24639

52 Fleming, M. D., Romano, M. A., Su, M. A., Garrick, L. M., Garrick, M. D. and Andrews, N. C. (1998) Nramp2 is mutated in the anemic Belgrade (b) rat: evidence of a role for Nramp2 in endosomal iron transport. Proc. Natl. Acad. Sci. U S A **95**, 1148-1153

53 Touret, N., Furuya, W., Forbes, J., Gros, P. and Grinstein, S. (2003) Dynamic traffic through the recycling compartment couples the metal transporter Nramp2 (DMT1) with the transferrin receptor. J. Biol. Chem. **278**, 25548-25557

ACKNOWLEDGEMENTS

We acknowledge Dr. Walter Schaffner for providing the 4xMRE(d) construct, and dr. P.J. van de Sluijs for providing pCL-NEO RabIP4-vsvG. We are grateful to Dr. Eric Kalkhoven and Prof. Dr. Cisca Wijmenga for critical evaluation of the manuscript, and the members the Klomp-Wijmenga group for valuable discussions and assistance. This work was supported by a grant from the Netherlands Organization for Scientific Research (NWO: 912-04-106).

FIGURE LEGENDS

Figure 1 Biochemical characterization of hCTR2

(**A**), Sequence alignment between hCTR1 and CTR2 from different species using the AlignX module from Vector NTI (Invitrogen). Identical (white text, black background), conserved (black text, grey background), and similar (white text, grey background) amino acids are indicated. The transmembrane regions (boxed regions) are indicated in Roman numericals. The MXXXM motif involved in copper coordination, the GXXXG motif involved in intra-helical interactions, and carboxy-terminal HCH motif are indicated. The Mets motifs and histidine rich regions involved in high affinity copper transport are underlined, and one conserved methionine residue is indicated by an asterisk. (**B**) Empty vector (EV), hCTR1-vsvG or hCTR2-vsvG constructs (lanes 1-3) were transiently transfected into HEK 293T cells prior to lysis. Immunoblot analysis was performed on proteins immunoprecipitated by anti-vsvG antibodies. (**C**) HEK 293T cells were transiently transfected with hCTR2-vsvG or EV (lane 1 and 2) constructs. Cells were incubated for 30 minutes at room temperature with increasing concentrations of the chemical cross-linker EGS (lanes 2-5). Immunoprecipitation and subsequent immunoblot analysis was performed to detect hCTR2-vsvG containing complexes (arrows). The heavy chain of the antibodies is marked with IgG. Apparent molecular masses are indicated on the left side of the immunoblots in kDa. (D) HEK 293T cells were transiently co-transfected with different constructs as indicated. Immunoprecipitation was performed with either mouse-anti-flag M2-agarose beads or rabbit-anti-vsvG attached to Protein A agarose beads. Precipitates were washed and separated by 12% SDS-PAGE and immunoblot analysis was performed with antibodies as indicated.

Figure 2 hCTR2 is localized in intracellular vesicles

(**A**) Localisation of hCTR2 was assessed by direct confocal laser scanning microscopy in HEK 293T, U2OS and HeLa cells after transient transfections with the hCTR2-eGFP construct. (**B**) HeLa cells were transiently co-transfected with hCTR2-vsvG and hCTR2-eGFP constructs. hCTR2-vsvG was immunolabelled with rabbit-anti-vsvG antibodies, and secondary labelling was performed with alexa568-conjugated antibodies. hCTR2-eGFP was visualized by direct confocal microscopy. Co-

localisation is indicated with arrowheads. Scalebars are presented in the right lower corners of all panels.

Figure 3 hCTR2 is partially colocalised with hCTR1

(**A**) Confocal laser scanning microscopy was performed on HeLa cells, which were transiently transfected with hCTR1-eGFP and hCTR2-vsvG constructs. hCTR2-vsvG was immunolabelled with rabbit-anti-vsvG antibodies, and secondary labelling was performed with alexa568-conjugated antibodies. hCTR1-eGFP was visualized by direct confocal microscopy. Plasmamembrane localisation of hCTR1-eGFP was indicated with arrows, and colocalisation with arrowheads. (**B**) HEK 293T cells were transiently transfected with the hCTR2-eGFP construct. Prior to analysis, cells were incubated for one hour with either the copper chelator bathocuproine disulphonic acid (BCS) or $CuCl_2$ in concentrations as indicated. Scalebars are presented in the right lower corners of all panels.

Figure 4 hCTR2 is colocalised with late endosomal and lysosomal vesicles

HEK 293T cells were transiently transfected with hCTR2-eGFP prior to labelling with antibodies against different vesicular markers: the trans-Golgi network marker p230, the transferrin receptor for early endosomes, CD63 for late endosomes, and lysosomal markers LAMP-1 and LAMP-2, and secondary labelling was performed with alexa568 conjugated antibodies. Visualization was performed as in figure 2. Green and red channels were merged to determine co-localisation (arrowheads). Scalebars are presented in the right lower corners of all panels.

Figure 5 Characterisation of a novel MRE-Luciferase reporter assay

(**A**) The MRE-Luciferase reporter was constructed by cloning four metal responsive elements (MRE) upstream of the Firefly Luciferase open reading frame of the pGL3-TATA construct. (**B**) HEK 293T cells were transiently transfected with the MRE-Luciferase reporter or the control vector pGL3-TATA. One day after transfection, cells were incubated for 24 hours with different $CuCl_2$ concentrations. (**C**) Metal toxicity was measured by MTT viability assays after incubation for 24 hours with different metal concentrations, and LD_{50} values were determined. (**D**) HEK 293T cells were transiently transfected with the MRE-Luciferase reporter, and one day after transfection cells were incubated with a low or a high sublethal metal concentration. (**E**) HEK 293T cells were transiently transfected with the MRE-Luciferase reporter or a HRE-Luciferase reporter. One day after transfection, cells were incubated with 100 μM $CuCl_2$ or 100 μM of the iron chelator desferoxamine (DFO) to mimic hypoxia. Luciferase reporter activities were measured and normalized for Renilla Luciferase activities. Values are expressed as fold induction relative to control incubations ± standard error of the mean as explained in Experimental Procedures. Figures represent at least three independent experiments.

Figure 6 Cellular copper uptake is facilitated by hCTR2 and is dependent on the CTR specific MXXXM motif

The MXXXM motifs were converted into IXXXI in pEBB-hCTR1-flag and pEBB-hCTR2-flag. HEK 293T cells were transiently transfected with the MRE-Luciferase reporter in combination with wildtype pEBB-hCTR1-flag (**A and B**), pEBB-hCTR2-flag (**C and D**) or their IXXXI mutants. One day after transfection, cells were incubated for 24 hours with increasing amounts of $CuCl_2$ (**A and C**) or $ZnCl_2$ (**B and D**). MRE-Luciferase reporter activities were measured and relative light units (RLU) were calculated after normalization for Renilla Luciferase activity. Values are expressed as fold induction relative to control incubations as explained in Experimental Procedures. Results are averages of at least three independent experiments assayed in triplicate ± standard error of the mean. Statistical differences between EV and hCTR1 or hCTR2 transfected cells were indicated (* = $p<0.01$). (**E**) Lysates from the MRE-Luciferase assay were dissolved in SDS-PAGE sample buffer, separated by SDS-PAGE and subjected to immunoblot analysis using mouse-anti-flag antibody.

Table 1. Primers

Name	Sequence (5'-3')
flagCullin1rev	tcacttgtcgtcatcgtcttgtagtcagccaagtaactgtaggtgtc
flagCullin1for	atggactacaaagacgatgacgacaagtcgtcaacccggagccag
hCTR2-vsvG fw	atggcgatgcatttcatctt
hCTR2-vsvG rev	tcactttcctagtcggttcatctcgatgtcagtgtaagctgtgctgagaagtgg
hCTR2 fw	atggcgatgcatttcatctt
hCTR2 rev	agctgtgctgagaagtgggt
4MRE-F/HindIII	cccaagcttgactcgaggagctctgcac
4MRE-R/PstI	ctgcagtatgccaaggtcgacgggc
hCTR2 BamHI fw	ctaggatccaccatggcgatgcatttcatcttc
hCTR2 NotI rev	gtaagcggccgcagctgtgctgagaagtgggtaag
hCTR1 BamHI fw	ggatccgccaccatggatcattcccaccatatg
hCTR1 NotI rev	gcggccgcatggcaatgctctgtgatatc
hCTR1 IXXXI fw	cataagctacttcctcattctcatcttcattacctacaacgggtac
hCTR1 IXXXI rev	gtacccgttgtaggtaatgaagatgagaatgaggaagtagcttatg
hCTR2 IXXXI fw	catcggctacttcatcattctggccgtaatttcctacaacacctg
hCTR2 IXXXI fw	caggtgttgtaggaaattacggccagaatgatgaagtagccgatg

Biochemical Journal Immediate Publication. Published on 6 Jul 2007 as manuscript BJ20070705

Figure 1.

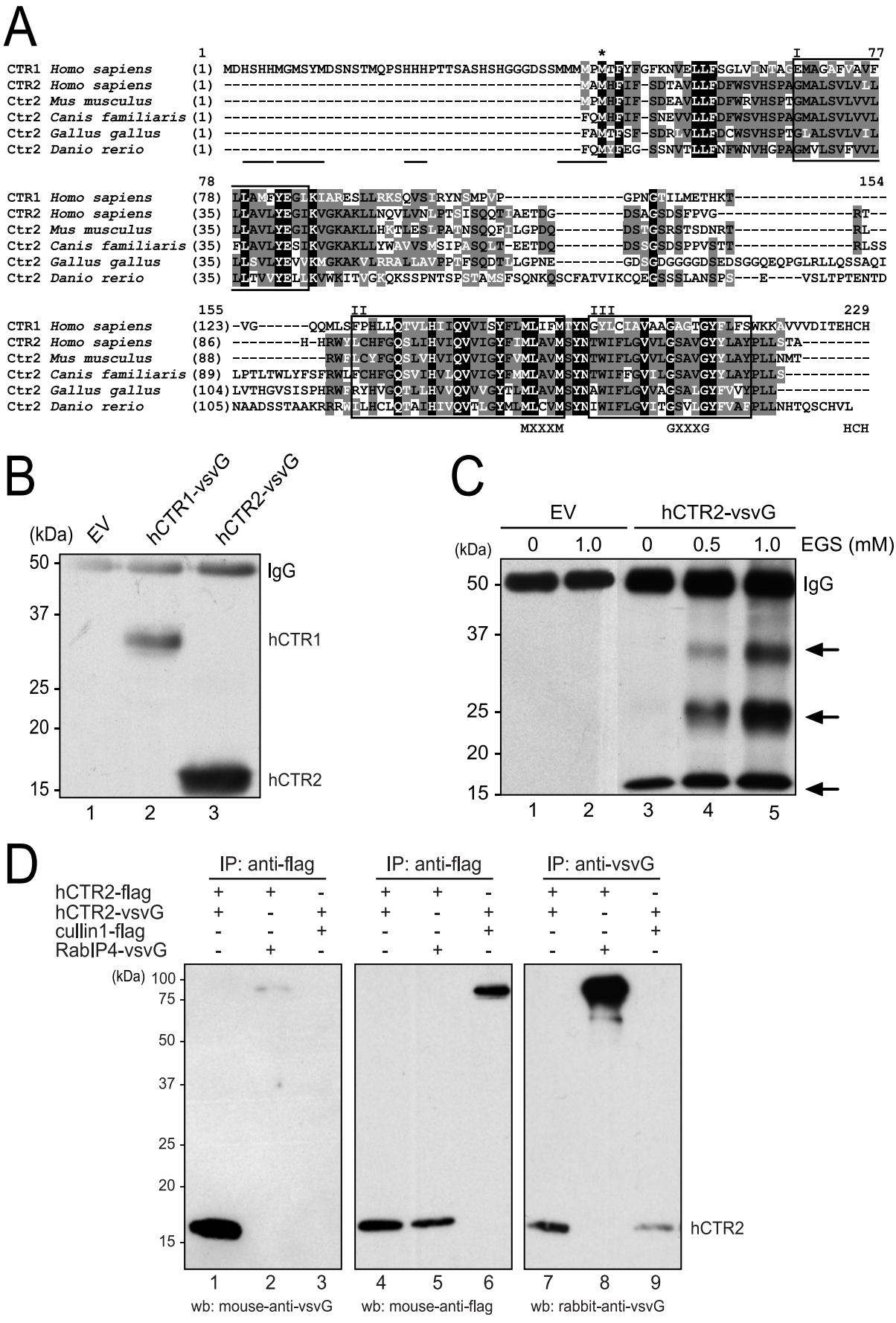

Biochemical Journal Immediate Publication. Published on 6 Jul 2007 as manuscript BJ20070705

Figure 2.

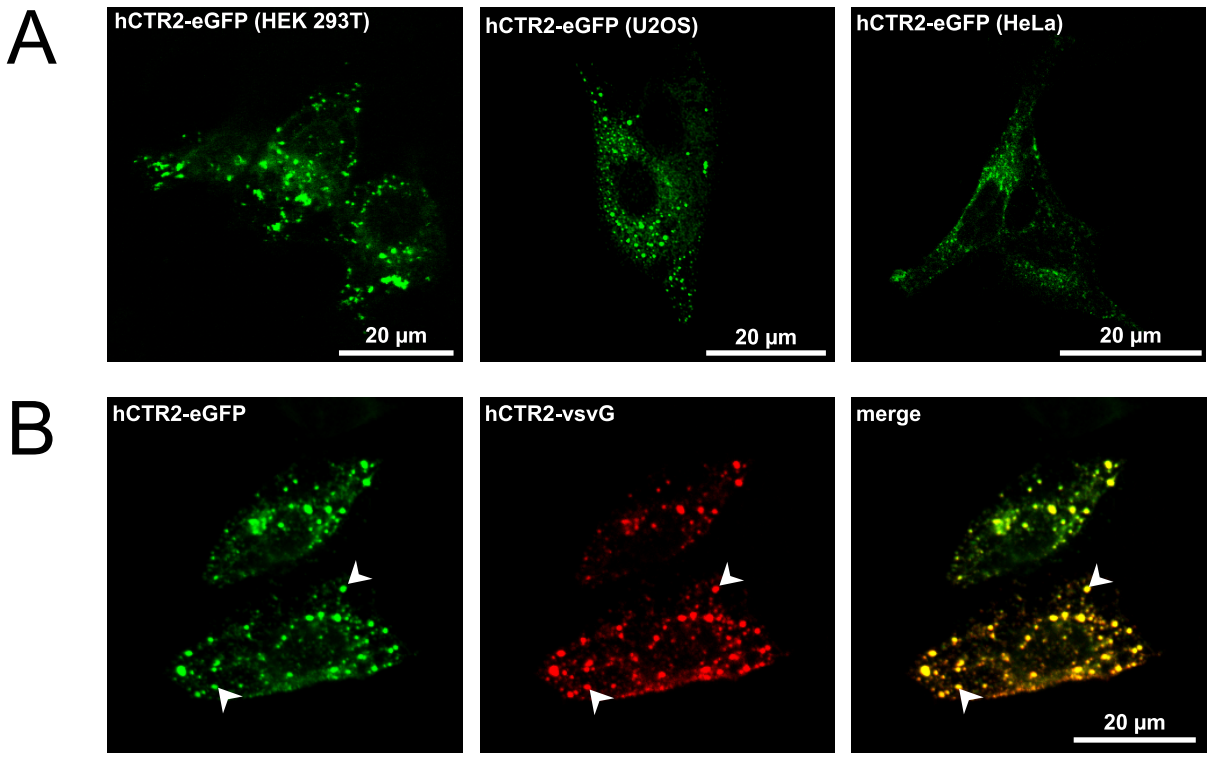

Biochemical Journal Immediate Publication. Published on 6 Jul 2007 as manuscript BJ20070705

Figure 3.

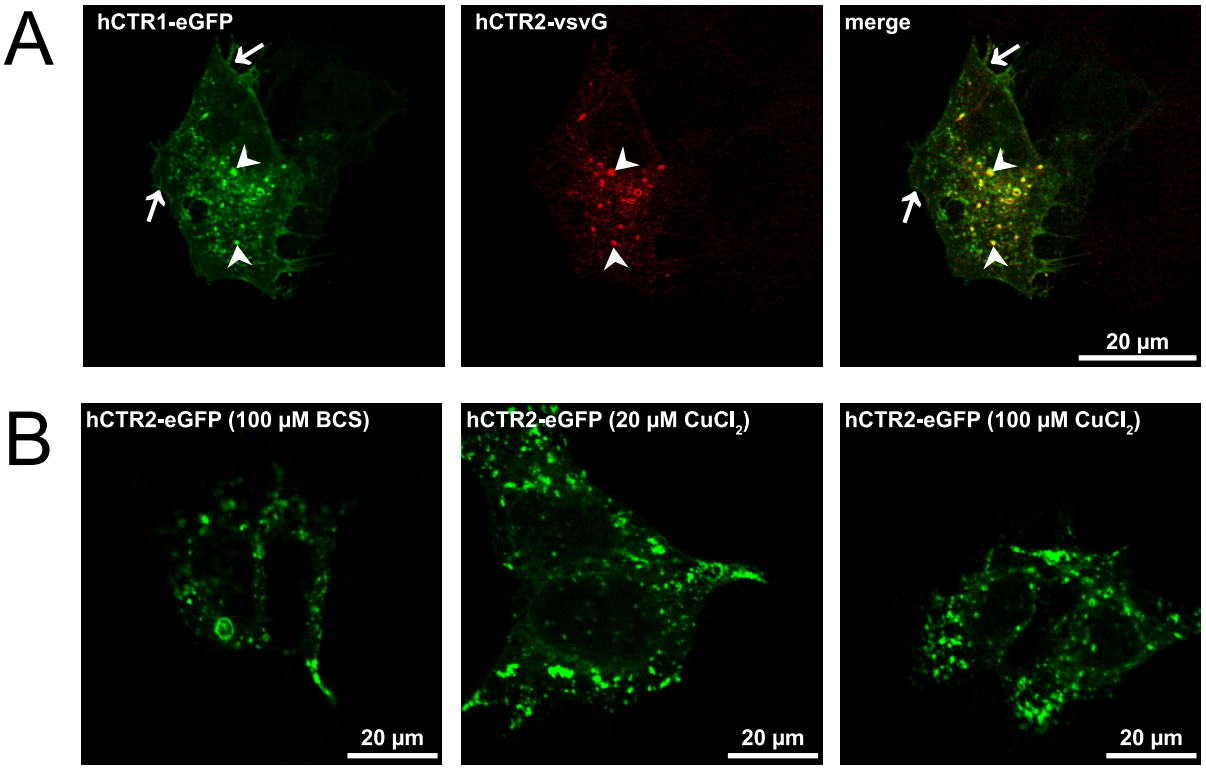

Biochemical Journal Immediate Publication. Published on 6 Jul 2007 as manuscript BJ20070705

Figure 4.

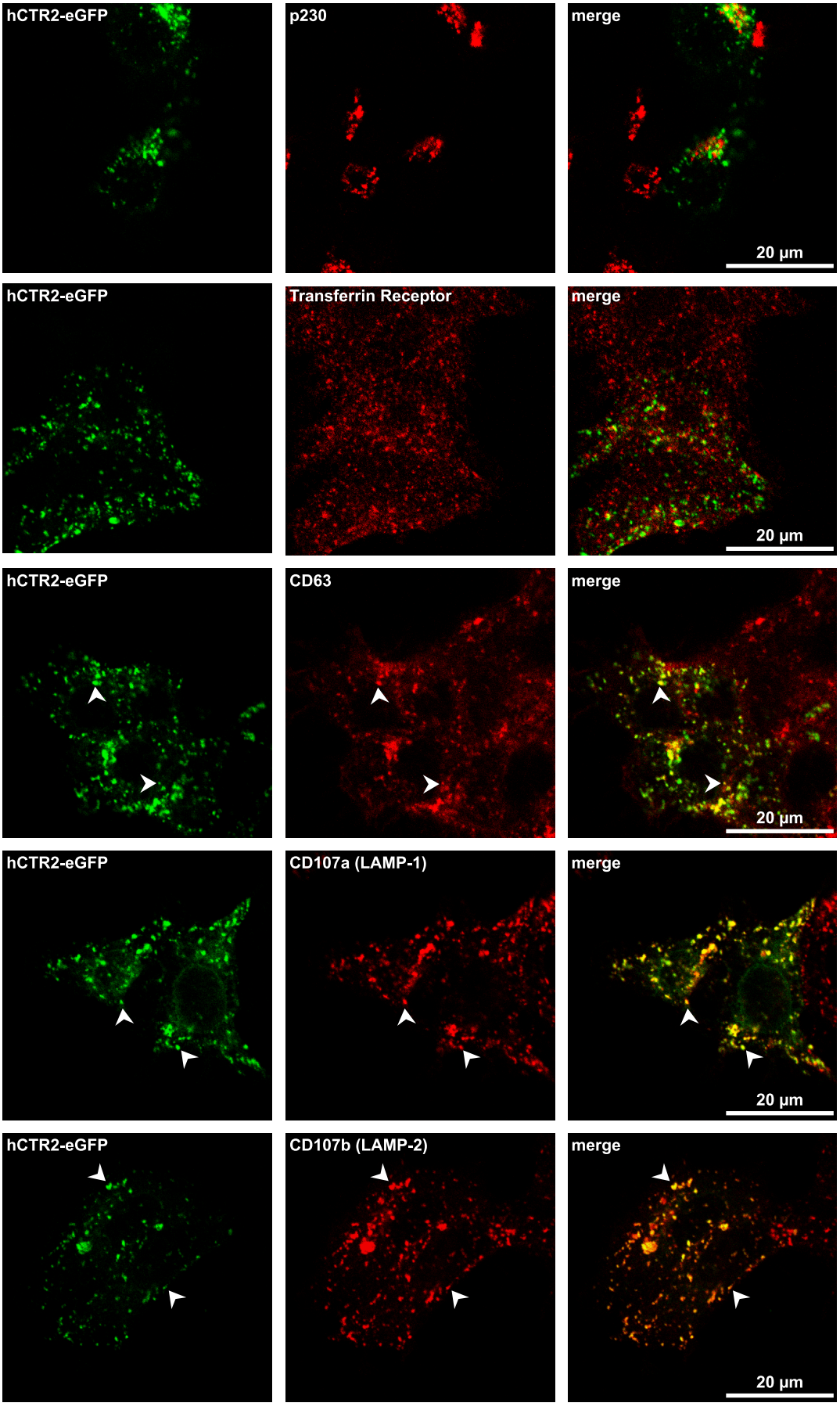

Biochemical Journal Immediate Publication. Published on 6 Jul 2007 as manuscript BJ20070705

Figure 5.

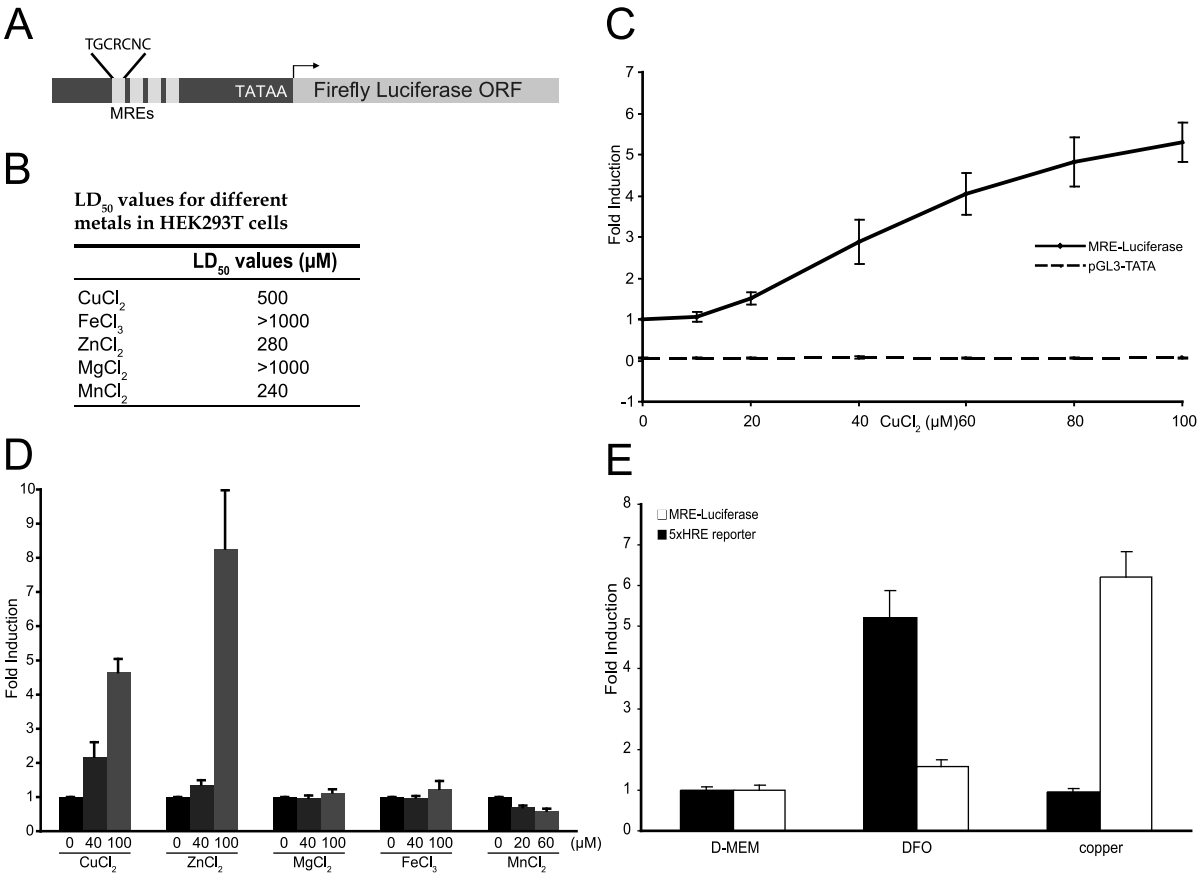

Biochemical Journal Immediate Publication. Published on 6 Jul 2007 as manuscript BJ20070705

Figure 6.